

Supplementary Materials for
**Metabolic traits shape responses to LSD1-directed therapy in glioblastoma
tumor-initiating cells**

Giulia Marotta *et al.*

Corresponding author: Giuliana Pelicci, giuliana.pelicci@ieo.it

Sci. Adv. **11**, eadt2724 (2025)
DOI: 10.1126/sciadv.adt2724

The PDF file includes:

Figs. S1 to S6
Tables S1 and S3
Legend for table S2

Other Supplementary Material for this manuscript includes the following:

Table S2

Figure S1

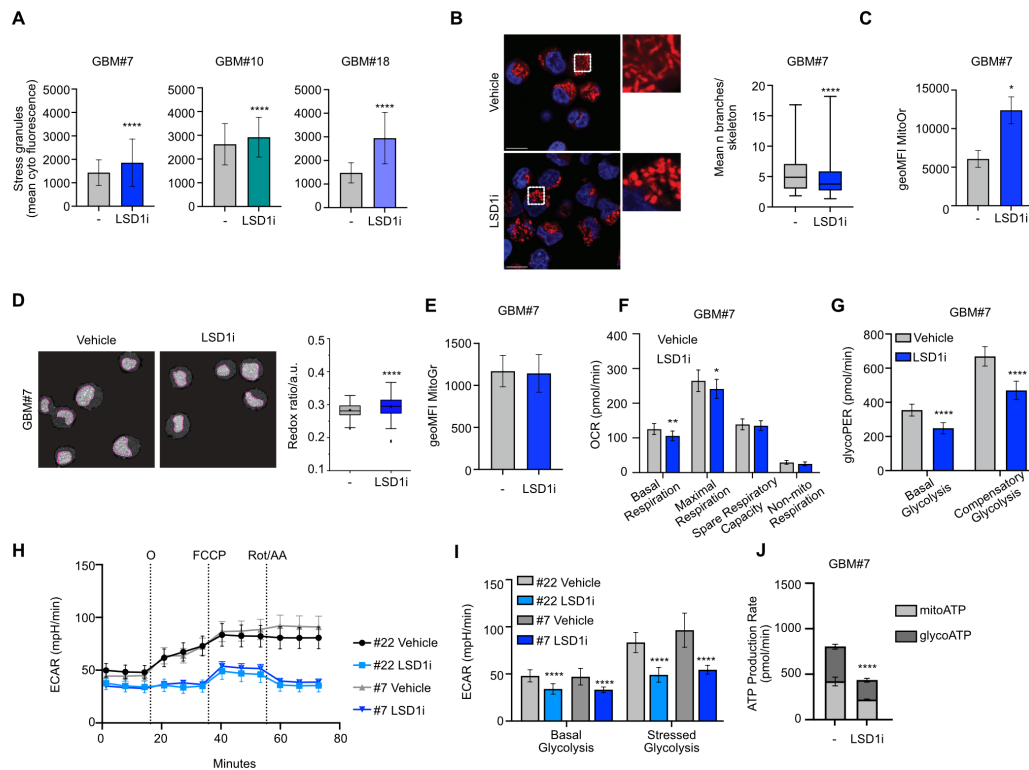
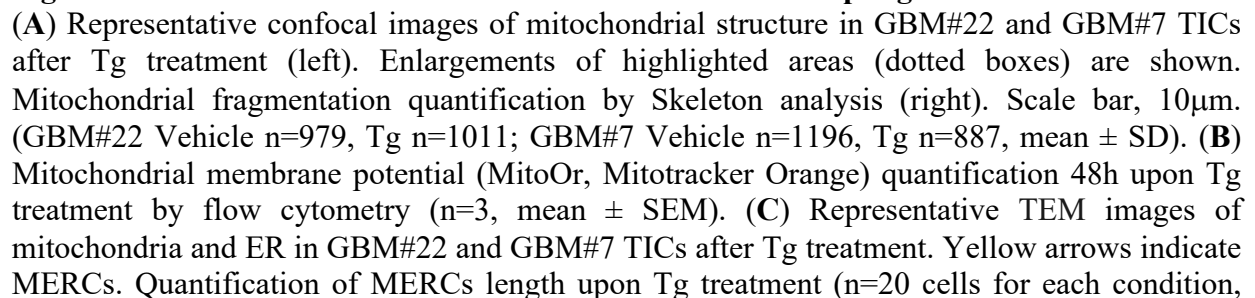


Figure S1. LSD1i treatment induces ISR and mitochondria perturbations in GBM TICs. (A) Quantification of G3BP1 signals (green) in the indicated GBM TICs upon LSD1i treatment. Actin filaments (Phalloidin, red) and DNA (DAPI, blue). Scale bar, 10 μ m (GBM#7 Vehicle n=5515, LSD1i n=3775; GBM#10 Vehicle n=2001, LSD1i n=3966; GBM#18 Vehicle n=2660, LSD1i n=5564 cells acquired, mean \pm SD). (B) Representative confocal images of mitochondrial structure in GBM#7 TICs after LSD1i treatment (left). Enlargement of the highlighted areas (dotted boxes) in the top right panel. Mitochondrial fragmentation quantification (right) by Skeleton analysis. Scale bar, 10 μ m. (n=2, mean \pm SD). (C) Mitochondrial membrane potential (MitoOr, Mitotracker Orange) quantification by flow cytometry (n=6, mean \pm SEM). (D) Representative images (left) and quantification (right) of redox ratio by TPEF microscopy in GBM#7 TICs after LSD1i treatment (Vehicle n=149, LSD1i n=167 cells acquired, mean \pm SD). (E) Mitochondrial mass (MitoGr, Mitotracker Green) quantification by flow cytometry (n=5, mean \pm SEM). (F) OCR by mitochondrial stress test in GBM#7 TICs after LSD1i: respiration parameters quantification (n=3, mean \pm SD). (G) Glycolytic proton efflux rate (glycoPER) by glycolytic rate assay in GBM#7 TICs post LSD1i: quantification of basal and compensatory glycolysis (n=3; mean \pm SD). (H) Extracellular acidification rate (ECAR) by Mitostress test in GBM#22 and GBM#7 TICs after LSD1i. Representative kinetic graph across time; lines indicate the addition of mitochondrial modulators oligomycin (O), Carbonyl cyanide-p-trifluoromethoxyphenylhydrazone (FCCP), and rotenone/antimycin A (Rot/AA). (I) Basal and stressed glycolysis quantification based on H profile (n=3, mean \pm SD). (J) Mitochondrial (mitoATP) and glycolytic ATP (glycoATP) production rate in GBM#7 TICs after LSD1i treatment by Seahorse XF Real-Time ATP Rate Assay (n=3 replicates/group, mean \pm SD). Two

tailed unpaired Student t test: *, $P < 0.05$; **, $P < 0.01$; ****, $P < 0.0001$ for (C, E and G, I and J); Mann–Whitney U test: ****, $P < 0.0001$ for (A, B, and D).

Figure S2. LSD1i increases functional ER-Mitochondrial coupling.



mean \pm SD). Scale bar 500nm. **(D)** Representative TEM images of mitochondria and ER in GBM#22 and GBM#7 TICs after LSD1i and Tg treatment. Enlargements of the highlighted areas (dotted boxes) shown on the right. Yellow arrows indicate MERCs. Scale bar 1 μ m and 200nm for the insert. Two tailed unpaired Student *t* test: *, $P < 0.05$ for B; Mann–Whitney *U* test: ****, $P < 0.0001$ for (A and C).

Figure S3

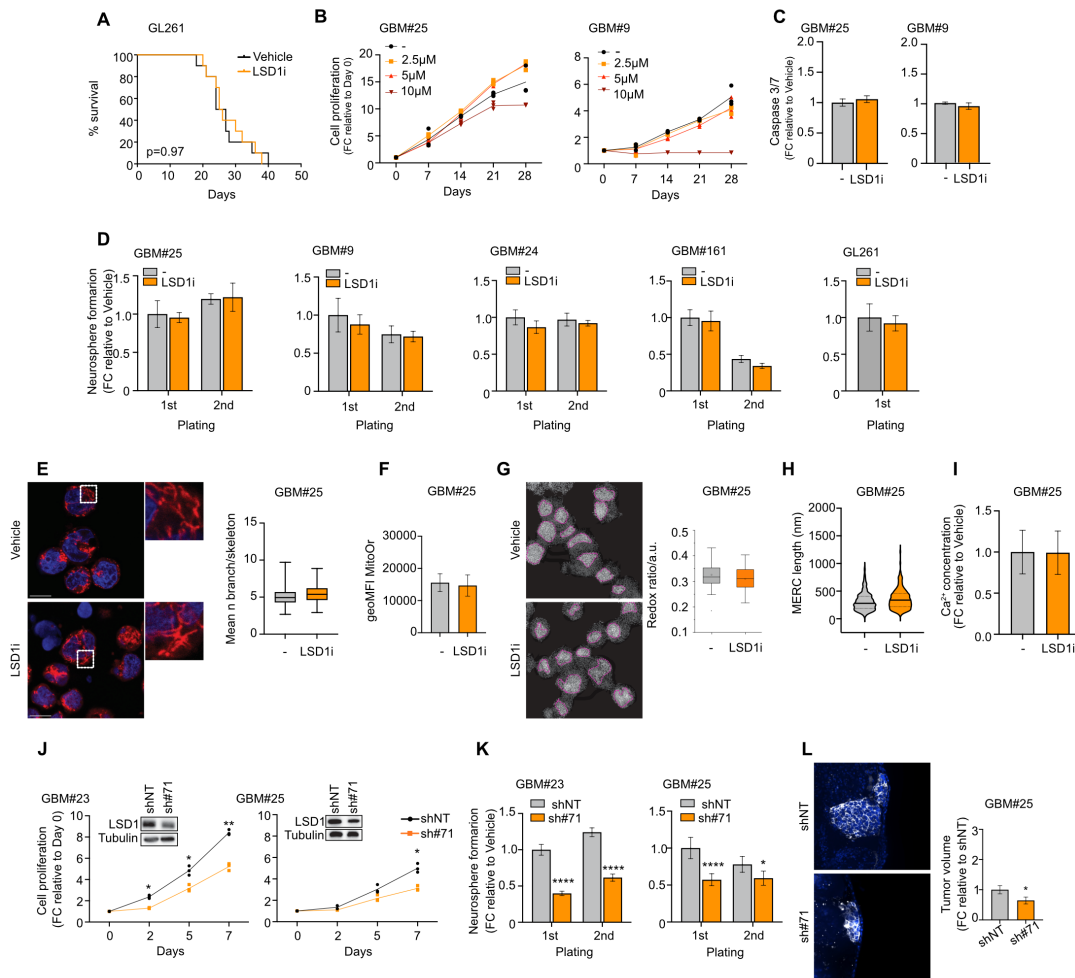


Figure S3. Inter-patient heterogeneity reveals TICs resistant to LSD1i treatment.

(A) Kaplan Meyer survival curve of mice transplanted with GL261 cells and treated with LSD1i. Treatment started 2 weeks post cell implantation. LSD1i was administered at 34mg/kg/o.s., twice a week for 4 weeks (n=10 vehicle and n=10 LSD1i). Survival differences by Log-rank test. (B) GBM#25 and GBM#9 growth after increasing LSD1i doses at indicated time points. LSD1i has been administrated every 7 days (n=3 replicates/group, mean \pm SD). (C) Caspase 3/7 activity in GBM#25 and GBM#9 treated with LSD1i or Vehicle control (n=3, mean \pm SD). (D) Neurosphere formation efficiency of GBM TICs treated with LSD1i or Vehicle control. Two serial neurosphere propagations were assessed. (n=3 GBM#9; n=2 GBM#25, GBM#24, GBM#161 and GL261, mean \pm SD). (E) Representative confocal images of mitochondrial structure in GBM#25 TICs after LSD1i treatment (left). Enlargements shown (dotted boxes). Mitochondrial fragmentation quantification by Skeleton analysis (right). Scale bar, 10 μ m (n=3, mean \pm SD). (F) Mitochondrial membrane potential (MitoOr, Mitotracker Orange) quantification by flow cytometry (n=6, mean \pm SD). (G) Representative images (left) and redox ratio quantification (right) by TPEF microscopy in GBM#25 TICs after LSD1i treatment (Vehicle n=215, LSD1i n=175 cells, mean \pm SD). (H) Quantification of MERCs length in GBM#25 TICs with and without LSD1i treatment (n=20 cells for each condition, mean \pm SD). (I) Measurements of Ca^{2+}

concentration by Rhod-2 fluorescence signals quantification in GBM#25 TICs after LSD1i treatment (n=3, mean \pm SD). **(J)** GBM#23 and GBM#25 growth after LSD1 silencing (sh#71) (n=3 replicates/group, mean \pm SD). LSD1 silencing efficiency (sh71) vs. scramble controls (shNT) in the corresponding samples evaluated by immunoblot (upper panel); Tubulin as loading control. **(K)** Neurosphere formation efficiency of GBM TICs after LSD1 silencing (sh#71). Two serial neurosphere propagations were assessed (n=3 replicates/group GBM#23; n=2 GBM#25, mean \pm SD). **(L)** Representative confocal images of embryonic zebrafish xenotransplanted with LSD1-silenced GBM#25 TICs. Tumor volume quantification is shown in the bar plot. Scale bar, 50 μ m. (shNT n=21, sh#71 n=22; mean \pm SEM). Two tailed unpaired Student *t* test: *, *P* < 0.05, for (C, D [GL261], F, I, and L); Mann–Whitney *U* test: for (E, G and H); ANOVA for (B, D, and J and K). FC, Fold Change.

Figure S4

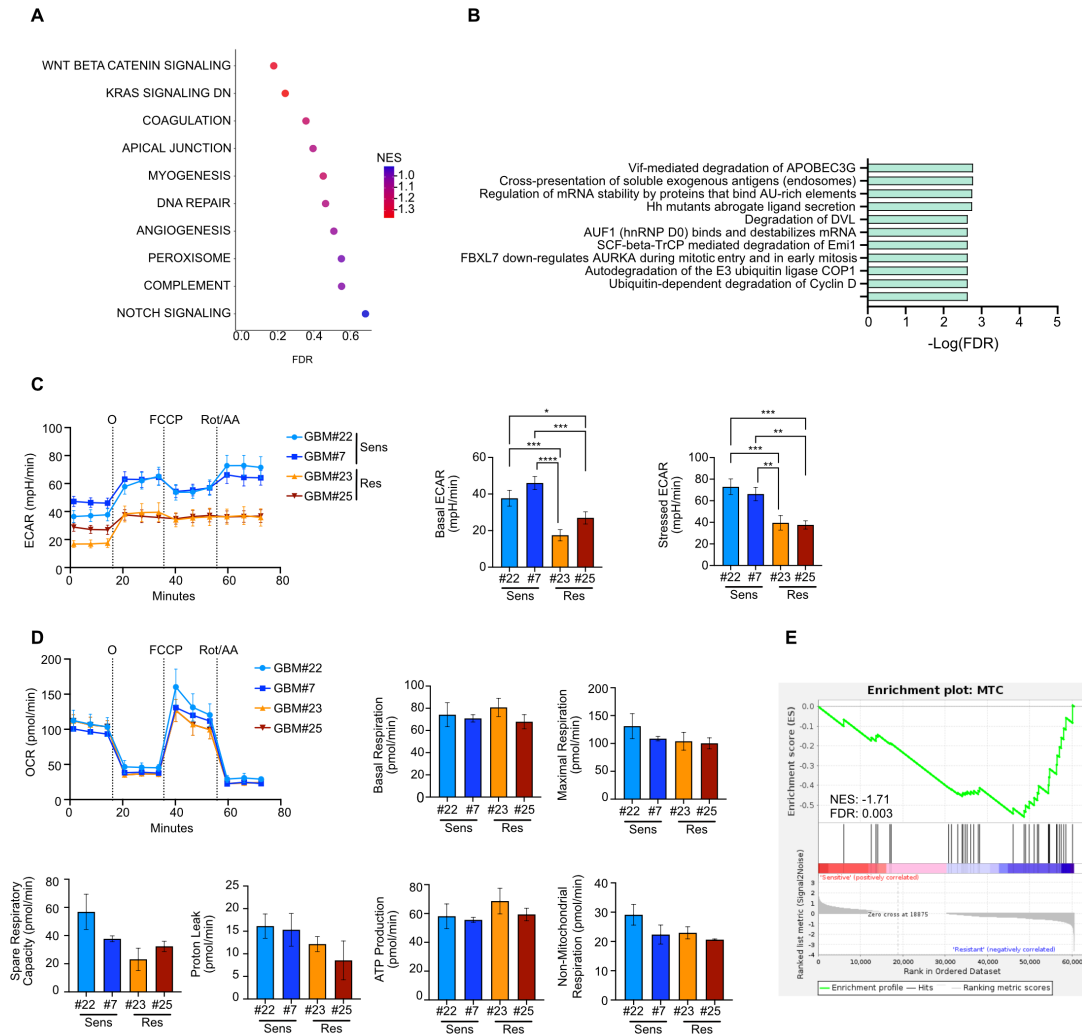


Figure S4. LSD1^{iSens} and LSD1^{iRes} TICs display different metabolic features.

(A) GSEA analysis of hallmark pathways downregulated in LSD1^{iSens} TICs (GBM#22, GBM#7, GBM#10, GBM#18, GBM#8) compared to LSD1^{iRes} TICs (GBM#23, GBM#9, GBM#24, GBM#161, GBM#53). The bubble color indicates the normalized enrichment score (NES); False Discovery Rate (FDR). (B) Pathway enrichment analysis of proteins significantly downregulated in LSD1^{iSens} TICs (GBM#22, GBM#7, GBM#10, GBM#18) compared to LSD1^{iRes} TICs (GBM#23, GBM#9, GBM#25). The top 10 terms (ranked by FDR) are shown. (C) Extracellular acidification rate (ECAR) by mitochondrial stress test in LSD1^{iSens} (GBM#22, GBM#7) and LSD1^{iRes} (GBM#23, GBM#25) TICs. Representative kinetic graph across time (left) with quantification of basal and stressed ECAR (right); lines indicate the addition of mitochondrial modulators oligomycin (O), Carbonyl cyanide-p-trifluoromethoxyphenylhydrazone (FCCP), and rotenone/antimycin A (Rot/AA) (n=3, mean \pm SD). (D) OCR by mitochondrial stress test in LSD1^{iSens} (GBM#22, GBM#7) and LSD1^{iRes} (GBM#23, GBM#25) TICs. Representative kinetic graph across time (left) and quantification of basal and maximal respiration, spare respiratory capacity, proton leak, ATP-linked OCR, and non-mitochondrial respiration (right) (n=3, mean \pm SD).

SD). Lines in the graph indicate the addition of mitochondrial modulators oligomycin (O), Carbonyl cyanide-p-trifluoromethoxyphenylhydrazone (FCCP), and rotenone/antimycin A (Rot/AA). (n=3, mean \pm SD). (E) GSEA enrichment plot of GBM mitochondrial subtype genes defined by Garofano and coworkers in LSD1i^{Res} TICs. ANOVA for (C and D).

Figure S5

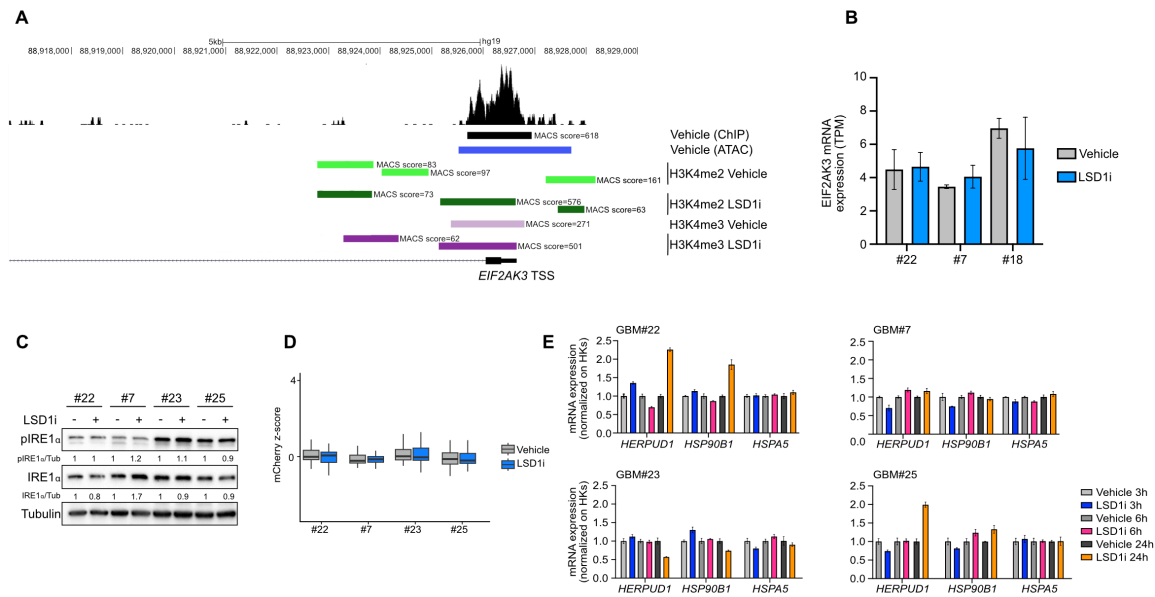


Figure S5. LSD1i induces PERK accumulation and alters PERK-mediated stress responses. (A) Promoter region of the *EIF2AK3* gene from UCSC Genome Browser, human hg19. The binding regions for LSD1, H3K4me2 and H3K4me3 in the GBM#22 TIC are shown, with corresponding MACS scores. (B) Bar plot reporting the expression level of *PERK* mRNA in terms of TPMs (Transcripts Per Million) in various GBM TICs treated or not with LSD1i. For each cell line and condition, biological replicates have been merged and only the average TPM between replicates is reported. (C) Representative immunoblot analysis of pIRE1α/IRE1α and Tubulin (loading control) in LSD1i^{Sens} (GBM#22, GBM#7) and LSD1i^{Res} (GBM#23, GBM#25) TICs after LSD1i treatment (n=3). Protein levels normalized to Tubulin and expressed as fold change relative to untreated TIC. (D) Representative bar plot of mean mCherry fluorescence intensity in the indicated GBM TICs after LSD1i treatment (n=2) (E) Relative mRNA expression of ATF6 target genes in TICs after LSD1i treatment. All data were normalized to geometric mean of housekeeping genes including *TBP*, *GAPDH*, *RPLPO*, and *18S* (n=3 replicates/group, mean ± SD).

Figure S6

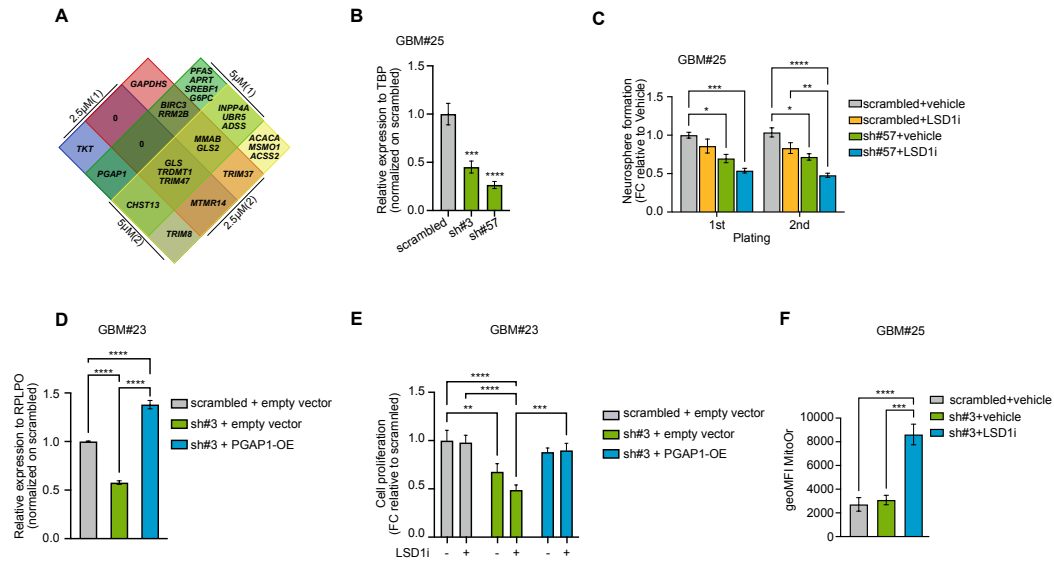


Figure S6. PGAP1 is a key mediator of LSD1i resistance.

(A) Venn diagram showing shared and unique depleted genes across treatment conditions. (B) *PGAP1* silencing efficiency (sh#3 and sh#57) in GBM#25 TICs compared control (scrambled) evaluated by RT-qPCR; *TBP* used for normalization. (C) Neurosphere formation efficiency of GBM#25 TICs assessed after *PGAP1* silencing (sh#57) in combination with LSD1i treatment. Two serial neurosphere propagations assessed (n=3, mean \pm SD). (D) Rescue of *PGAP1* expression (sh#3 + *PGAP1*-OE) in *PGAP1*-silenced (sh#3 + empty vector) cells compared to control (scrambled + empty vector) GBM#23 TICs assessed by RT-qPCR (n=3 replicates/group, mean \pm SD); *RPLPO* used for normalization. (E) Growth of GBM#23 TICs as in D, measured after 7 days of LSD1i treatment (n=2, mean \pm SD). (F) Mitochondrial membrane potential (MitoOr, Mitotracker Orange) quantification in *PGAP1*-silenced GBM#25 TICs (sh#3) as in (B) after LSD1i treatment. (n=4, mean \pm SEM). Two tailed unpaired Student *t* test: ***, $P < 0.001$; ****, $P < 0.0001$ for B. ANOVA: *, $P < 0.05$; **, $P < 0.01$, ***, $P < 0.001$; ****, $P < 0.0001$ for (C-F).

Table S1. Clinical and molecular data of GBM TICs.

	GBM#9	GBM#161	GBM#20	GBM#153	GBM#25
Tumor Type	GBM	GBM	GBM	GBM	GBM
Surgery	II	I	I	II	II
Sex	F	M	M	M	M
TP53	WT	mut	mut	WT	mut
EGFR	WT	WT	WT	WT	WT
PDGFRA	WT	WT	WT	WT	WT
PTEN	del	n.d.	WT	WT	WT
PI3KCA	WT	WT	WT	WT	WT
CDKN2A	WT	WT	WT	WT	WT
IDH1	n.a.	WT	n.a.	n.a.	n.a.
NOTCH1	WT	mut	WT	WT	WT
ATRX	WT	WT	WT	WT	WT
BRAF	mut	WT	WT	WT	WT
NF1	mut	WT	WT	WT	WT
MGMT	n.a.	M	n.a.	n.a.	n.a.

For each LSD1^{iRes} GBM TIC, sample type (I and II surgery), the sex (male [M] or female [F]) of the patient from which the GBM TIC culture was derived, and the mutation status of each gene are indicated.

GBMWT: wild-type; mut: mutant; M: methylated; del: deletion, n.d.: not determined, n.a.: not available.

Table S2. Analysis of the metabolic library screening (separate file).

Excel file containing the metabolic library screening gene list (10 shRNA per gene) and the criteria applied to obtain the putative synthetic lethality genes in combination with LSD1i treatment, related to Figures 7 and S6.

Table S3. Primer list.**SYBR Green assays**

Gene name	Forward (5'-3')	Reverse (5'-3')
<i>TBP</i>	TGCACAGGAGCCAAGAGTGAA	CACATCACAGCTCCCCACCA
<i>XBP1t</i>	TGCCAGAGATCGAAAGAAGGC	GCGCTGTCTTAACTCCTGGTT
<i>XBP1s</i>	CCCTGGTTGCTGAAGAGGAG	CTGCACCTGCTGCGGAC
<i>XBP1u</i>	CCGCAGCACTCAGACTACG	TGTCCAGAATGCCCAACAGG
<i>PGAP1</i>	ACTTGTGGAGCACTAGCCAT	AGCTGGCTTGACAGATGAACA
<i>DDIT3</i>	GGAAACAGAGTGGTCATTCT	CTGCTTGAGCCGTTTCATTCT
<i>CHAC1</i>	GTGTGGTGACGCTCCTTGAAGA	TGCTCCCCTTGCACTTGGTAT
<i>ATF3</i>	CTCGGGGTGTCCATCACAAAAG	AGCTTCTCCGACTCTTTCTGC
<i>GAPDH</i>	AGCCACATCGCTCAGACAC	GCCCAATACGACCAAATCC
<i>RPLP0</i>	TTCATTGTGGGAGCAGAC	CAGCAGTTTCTCCAGAGC
<i>18S</i>	CGCCGCTAGAGGTCAAATTC	CTTTCGCTCTGGTCCGTCTT

TaqMan assays

Gene Name	Taqman reference number
<i>ATF3</i>	Hs00231069_m1
<i>CHAC1</i>	Hs00225520_m1
<i>DDIT3</i>	Hs00358796_g1
<i>HERPUD1</i>	Hs01124269_m1
<i>HSP90B1</i>	hs00427665_g1
<i>HSPA5</i>	Hs00607129_gH
<i>PGAP1</i>	Hs01088726_m1
<i>GAPDH</i>	hs99999905_m1
<i>RPLP0</i>	hs99999902_m1
<i>18S</i>	Hs99999901_s1
<i>TBP</i>	hs99999910_m1